EPJ manuscript No.
(will be inserted by the editor)

Quantitative theory of channeling particle diffusion in transverse energy in the presence of nuclear scarrering and direct evaluation of dechanneling length

Victor V. Tikhomirov

Institute for Nuclear Problems, Belarusian State University, Minsk

Received: date / Revised version: date

Abstract. A refined equation for channe;ing particle diffusion in transverse energy taking into consideration large-angle scattering by nuclei is suggested. This equation is reduced to the Sturm-Liouville problem allowing one to reveal both the origin and the limitations of the dechanneling length notion. The values of the latter is evaluated for both positively and negatively charged particles of various energies. It is also demonstrated that the dechanneling length notion is inapplicable for the nuclear dechanneling process of positively charged particles, while the effective electron dechanneling length of the latter vary more than twice converging to a constant assymptotic value at the depth exceeding the latter.

PACS. 61.85.+p Channeling phenomena (blocking, energy loss, etc.) – 25.40.Cm Elastic proton scattering

arXiv:1701.05235v1 [physics.acc-ph] 18 Jan 2017

1 Introduction

Channeling effect in crystals delivers unique possibilities of both high energy charged particle radiation and control. Both electron and positron channeling makes it possible to devise the new semi-monochromatic sources of x- and γ-radiation [1,2,3]. Proton and ion planar channeling in bent crystals is a promising tool for both extraction and collimation of the beams of the Large hadron collider (LHC) and Future circular collider (FCC) [4,5,6]. Planar channeling of charmed and beauty baryons in bent crystals also makes it possible to study the effects of both CP- and CPT violation [7].

All the applications of channeling effect are limited by its instability, induced by the dechanneling process. To describe the latter, a concept of particle diffusion in the energy of its transverse motion (transverse energy) was suggested soon after the channeling discovery [8,9,10].

The dechanneling process is often characterized by the visual notion of dechanneling length. Some information concerning the latter can be extracted from Monte Carlo simulations. However, since the average dechanneling distance of an individual particle strongly depends on its initial transverse energy, any direct method of dechanneling length evaluation through either the channeling fraction or dechanneling distance averaging over the incident particle angular distribution will give a result depending on the latter. In addition, there is no ground to expect that a channeling fraction, evaluated by any averaging method, will exponentially depend on the particle penetration depth, justifying an introduction of a dechanneling length independent of the latter.

In fact, only the theory [10], describing the collective properties of statistical particle behavior and consisting in finding the lowest eigen number of the diffusion equation, can be used for both strict introduction and evaluation of the dechanneling length. Since the dechanneling lengths of positively charged particles reach meters and tens of them at the LHC and FCC energies, the direct method [10] of their evaluation is more superior than the Monte Carlo simulations which become time consuming in the TeV particle energy region.

The theory [10] is applicable only in the case of electron dechanneling of nonrelativistic ions. Since the maximal angle $\theta_{max} = m/M$ of scattering by electrons considerably exceeds the critical channeling angle of nonrelativistic ions, the electron dechanneling of the latter can be correctly described in neglect of both large-angle catastrophic scattering and the scattering angle fourth power contribution to the mean square variation of transverse energy. However, these assumptions loose their applicability in many other cases.

First of all, since the channeling angle decreases with energy becoming much less than $\theta_{max} = m/M$, the modification [13,5] of the theory [10] for the ultrarelativistic case does not take into consideration adequately the particle scattering by crystal atom electrons. Also nuclear scattering both limits the fraction of channeling positively charged particles and is essential for channeling of negatively charged ones, considerably complicating the latter by the rechanneling process [11,12].

Send offprint requests to: Victor V. Tikhomirov

Recently the experiments with bent crystals were first conducted to separate the nuclear dechanneling process of both positively [14,15] and negatively [16] charged particles. The observed dechanneling fraction was fitted by the exponential decay law being necessary to introduce a constant nuclear dechanneling length. However, neither a justification of introduction nor a way of evaluation of the latter were suggested in [14,15,16].

To provide a correct evaluation of the dechanneling length in the presence of nuclear scattering, an improved diffusion equation, which takes into consideration both the scattering angle fourth power contribution to the mean square variation of transverse energy and large-angle catastrophic scattering, is introduced in this paper. This equation is used to evaluate to dechanneling length for the largest accelerator energies as well as to reveal the peculiarities of the dechanneling process introduced by both nuclear and electron scattering of both positively and negatively charged particles.

2 Refined equation for channeled particle diffusion in transverse energy

2.1 New features of the diffusion equation in transverse phase space

According to the Lindhard averaged potential concept [1, 5,8,9], particle motion at small angles with respect to crystal planes is described by the averaged atomic potential $V(x)$ (potential energy, see Fig. 1) which translation symmetry justifies the introduction of the conserving energy of transverse motion [1]

$$\varepsilon_\perp = \varepsilon v_x^2/2 + V(x) = p_x^2/2\varepsilon + V(x), \tag{1}$$

or transverse energy for short, in which ε is total particle energy, $p_x = \varepsilon v_x$ and $v_x(\varepsilon_\perp, x) = \sqrt{2\left[\varepsilon_\perp - V(x)\right]/\varepsilon}$ are, respectively, its momentum and velocity projections on the x axis normal to the crystal planes. Conservative particle motion in the potential V(x) is always disturbed by the incoherent scattering by both nuclei and electrons – see Fig. 1. At that, an instant incoherent deflection by the angle θ_x in the point x induces a transverse energy change from (1) to

$$\varepsilon'_\perp = \varepsilon[v_x(x)+\theta_x]^2/2+V(x) = \varepsilon_\perp+\varepsilon v_x(x)\theta_x+\varepsilon\theta_x^2/2. \tag{2}$$

To describe the cumulative result of such changes, Fokker-Planck approximation [1,5,17,18], which, is able to treat small transverse energy changes only [10,5,18], is widely applied. Following the well established procedure [17] and using the notations of [18], one can introduce a distribution function in the one dimensional transverse phase space

$$F(\varepsilon_\perp, x, z) = \varphi(\varepsilon_\perp, z) f_{\varepsilon_\perp}(x) \tag{3}$$

and the same over the transverse energy

$$\varphi(\varepsilon_\perp, z) \equiv \frac{1}{N}\frac{dN}{d\varepsilon_\perp}, \tag{4}$$

[1] The system of units $\hbar = c = 1$ is used.

where

$$f_{\varepsilon_\perp}(x) = \frac{2}{T\, v_x(\varepsilon_\perp, x)}. \tag{5}$$

is the coordinate space distribution function in which

$$T(\varepsilon_\perp) = 2\int\limits_{x_l(\varepsilon_\perp)}^{x_r(\varepsilon_\perp)} \frac{dx}{v_x(\varepsilon_\perp, x)}, \tag{6}$$

$x_l(\varepsilon_\perp)$ and $x_r(\varepsilon_\perp)$ are the period and the right and left turning points of the channeling motion at given $\varepsilon_\perp$. The dependence of the phase space distribution function (3) on the depth z of particle penetration into the crystal along the channeling planes is governed by the equation

$$\frac{\partial F}{\partial z} = -\frac{\partial}{\partial \varepsilon_\perp}\left(\frac{\Delta\varepsilon_\perp}{\Delta z}F\right) + \frac{1}{2}\frac{\partial^2}{\partial \varepsilon_\perp^2}\left(\frac{(\Delta\varepsilon_\perp)^2}{\Delta z}F\right) - wF, \tag{7}$$

$$\frac{\Delta\varepsilon_\perp}{\Delta z} = \frac{\Delta\varepsilon_\perp(\varepsilon_\perp, x)}{\Delta z} = \int(\varepsilon'_\perp - \varepsilon_\perp)d\Sigma, \tag{8}$$

$$\frac{(\Delta\varepsilon_\perp)^2}{\Delta z} = \frac{(\Delta\varepsilon_\perp)^2\,(\varepsilon_\perp, x)}{\Delta z} = \int(\varepsilon'_\perp - \varepsilon_\perp)^2 d\Sigma, \tag{9}$$

which was deduced following [18] and supplemented here for the first time by the last term, which contains the probability

$$w = w\,(\varepsilon_\perp, x) = \int' d\Sigma \tag{10}$$

of "catastrophic" scattering and describes the single scattering process of particle immediate knocking out from the channeling state. Another new feature will be the preservation of the forth scattering angle power contribution to the integrand of Eq. (9), to introduce which a specific definition of the integral regions of Eq. (8) -(10) is introduced below.

To make the consideration more transparent, we will use the simplified expression for the particle macroscopic scattering cross section on both nuclei with local number density $n_n(x)$ and electrons with local number density $n_e(x)$:

$$d\Sigma = \frac{4\alpha^2[Z^2 n_n(x) + n_e(x)]}{\beta^2 p^2(\theta^2+\theta_1^2)^2} d\theta_x d\theta_y, \tag{11}$$

where θ_1 is the angle, which takes the atomic nucleus potential screening into consideration. Both $Z^2 n_n(x)$ and $n_e(x)$ coordinate dependence is illustrated by Fig. 1. The integrand of the mean-squared transverse energy variation rate (9)

$$(\varepsilon'_\perp - \varepsilon_\perp)^2 = 2\varepsilon\left[\varepsilon_\perp - V(x)\right]\theta_x^2 + \varepsilon^2\theta_x^4/4 + .., \tag{12}$$

in which the odd powers of the scattering angle θ_x are omitted, contains the fourth power contribution of the same, which has never been taken into consideration before [10,13,5]. The point is that, as can be directly seen from Eqs. (11) and (12), this contribution diverges at large θ_x and to treat it, finite integration limits should be introduced. To define them, the transverse energy (2) of the

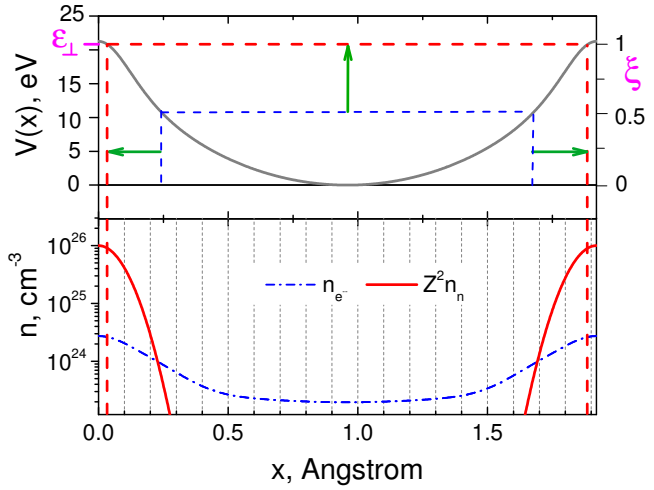

Fig. 1. Planar potential and the undertaken expansion of the considered region of positively charged particle motion, shown by arrows (top). Averaged number density of electrons and the same, multiplied the atomic number squared, of nuclei (bottom).

scattered particle has been equated to the height V_{max} of the planar potential.The boundary scattering angles which follows

$$\theta_{\pm}(\varepsilon_{\perp},x)=-v_x(\varepsilon_{\perp},x)\pm\sqrt{2\left(V_{max}-V(x)\right)/\varepsilon} \quad (13)$$

limit the integration region in Eq. (8) and (9) by the angles $\theta_-(\varepsilon_\perp,x)\le\theta_x\le\theta_+(\varepsilon_\perp,x)$, which leave the channeling particles channeled, and fix the complimentary integration regions $\theta_x>\theta_+(\varepsilon_\perp,x)$, $\theta_x<\theta_-(\varepsilon_\perp,x)$ in Eq. (10). The integration over all the angles $\theta_y=\sqrt{\theta^2-\theta_x^2}$ of scattering in the plane yz is assumed everywhere in Eqs. (8)-(10).

Given the integration limits explicitly determined, the integrals (8)-(10) can be routinely taken with the result

$$\begin{aligned}&\tfrac{\Delta\varepsilon_\perp(\varepsilon_\perp,x)}{\Delta z}=\tfrac{\pi\alpha^2}{\beta^3p}[Z^2n_n(x)+n_e(x)]\\&\times\left\{\ln\left[\tfrac{\theta_+(x)+\sqrt{\theta_+^2(x)+\theta_1^2}}{\theta_-(x)+\sqrt{\theta_-^2(x)+\theta_1^2}}\right]\right.\\&\left.+\tfrac{\theta_-(x)}{\sqrt{\theta_-^2(x)+\theta_1^2}}-\tfrac{\theta_+(x)}{\sqrt{\theta_+^2(x)+\theta_1^2}}\right\}\end{aligned} \quad (14)$$

for the rate of transverse energy variation growth;

$$\frac{(\Delta\varepsilon_\perp)^2(\varepsilon_\perp,x)}{\Delta z}=a(\varepsilon_\perp,x)+b(\varepsilon_\perp,x), \quad (15)$$

where

$$a(\varepsilon_\perp,x)=4\left[\varepsilon_\perp-V(x)\right]\frac{\Delta\varepsilon_\perp}{\Delta z} \quad (16)$$

and

$$\begin{aligned}&b(\varepsilon_\perp,x)=\tfrac{\pi\alpha^2}{4}[Z^2n_n(x)+n_e(x)]\\&\times\left\{\theta_+(x)\sqrt{\theta_+^2(x)+\theta_1^2}-\theta_-(x)\sqrt{\theta_-^2(x)+\theta_1^2}\right.\\&+\tfrac{2\theta_1^2\theta_+(x)}{\sqrt{\theta_+^2(x)+\theta_1^2}}-\tfrac{2\theta_1^2\theta_-(x)}{\sqrt{\theta_-^2(x)+\theta_1^2}}\\&\left.-3\theta_1^2\ln\left[\tfrac{\theta_+(x)+\sqrt{\theta_+^2(x)+\theta_1^2}}{\theta_-(x)+\sqrt{\theta_-^2(x)+\theta_1^2}}\right]\right\}\end{aligned} \quad (17)$$

for the rate of squared transverse energy variation growth and

$$\begin{aligned}&w(\varepsilon_\perp,x)=\tfrac{\pi\alpha^2}{\beta^2p^2\theta_1^2}[Z^2n_n(x)+n_e(x)]\\&\times\left\{2+\tfrac{\theta_-(x)}{\sqrt{\theta_-^2(x)+\theta_1^2}}-\tfrac{\theta_+(x)}{\sqrt{\theta_-^2(x)+\theta_1^2}}\right\}\end{aligned} \quad (18)$$

for the catastrophic scattering probability.

2.2 Reduction of the diffusion equation to the transverse energy space

To reduce the diffusion equation (7) in the transverse phase space to that in the transverse energy space, the averaging over the period of transverse motion

$$\langle\Phi(\varepsilon_\perp,x)\rangle=\int\limits_{x_l(\varepsilon_\perp)}^{x_r(\varepsilon_\perp)}\Phi(\varepsilon_\perp,x)f_{\varepsilon_\perp}(x)dx \quad (19)$$

is used [18] resulting in equation

$$\begin{aligned}&\tfrac{\partial\varphi(\varepsilon_\perp,z)}{\partial z}=-\tfrac{\partial}{\partial\varepsilon_\perp}\left(A(\varepsilon_\perp)\tfrac{\partial}{\partial\varepsilon_\perp}\tfrac{\varphi(\varepsilon_\perp,z)}{T(\varepsilon_\perp)}\right)\\&+\tfrac{\partial^2}{\partial\varepsilon_\perp^2}\left(B(\varepsilon_\perp)\tfrac{\varphi(\varepsilon_\perp,z)}{T(\varepsilon_\perp)}\right)-W(\varepsilon_\perp)\varphi(\varepsilon_\perp,z),\end{aligned} \quad (20)$$

containing the averaged coefficients

$$\begin{aligned}A(\varepsilon_\perp)&=\left\langle\tfrac{\Delta\varepsilon_\perp(\varepsilon_\perp,x)}{\Delta z}\right\rangle,\\B(\varepsilon_\perp)&=\langle b(\varepsilon_\perp,x)\rangle,\\W(\varepsilon_\perp)&=\langle w(\varepsilon_\perp,x)\rangle.\end{aligned} \quad (21)$$

Eq. (20) suggests, instead of transverse energy, to introduce both the variable

$$\xi'(\varepsilon_\perp)=\int\limits_0^{\varepsilon_\perp}T(\varepsilon_\perp)d\varepsilon_\perp, \quad (22)$$

and corresponding distribution function

$$u(\xi)=\frac{\varphi(\varepsilon_\perp)}{T(\varepsilon_\perp)}=\frac{1}{N}\frac{dN}{T(\varepsilon_\perp)d\varepsilon_\perp}=\frac{1}{N}\frac{dN}{d\xi'}. \quad (23)$$

The variable (22) has a clear semiclassical meaning, being equal to the multiplied by 2π quantum number of transverse oscillatory motion in the state corresponding to the considered transverse energy $\varepsilon_\perp$. Both Eqs. (22), (23) and the standard transformations [19] allows one to extract further the Sturm-Liouville operator in Eq. (20)

$$r(\xi')\frac{\partial u(\xi',z)}{\partial z}=\frac{\partial}{\partial\xi'}\left(p'(\xi')\frac{\partial u(\xi',z)}{\partial\xi'}\right)-q(\xi')u(\xi',z)\,, \quad (24)$$

with the coefficients

$$p'(\xi')=\left[B\left(\varepsilon_\perp(\xi')\right)+A\left(\varepsilon_\perp(\xi')\right)\right]T\left(\varepsilon_\perp(\xi')\right)r(\xi'), \quad (25)$$

$$q(\xi')=\left[W\left(\varepsilon_\perp(\xi')\right)-B''\left(\varepsilon_\perp(\xi')\right)\right]T^{-1}\left(\varepsilon_\perp(\xi')\right)r(\xi') \quad (26)$$

and

$$r(\xi') = \exp \int_0^{\varepsilon_\perp(\xi')} \frac{B'(\varepsilon_\perp)d\varepsilon_\perp}{A(\varepsilon_\perp)+B(\varepsilon_\perp)} ,$$
$$\varepsilon_\perp(\xi') = \int_0^{\xi'} \frac{d\xi}{T(\varepsilon_\perp(\xi))} , \quad (27)$$

which can be readily calculated using Eqs. (14)-(19) and (21). It should be emphasised that Eq. (24) is more general than that used in [10,13], which follows from Eq. ((24) at $q = 0$ and $r = const$.

2.3 Diffusion equation boundary conditions

Introducing the boundary conditions for Eq. (24), we immediately adopt the one of $\partial u(0)/\partial\xi' = 0$, reflecting the impossibility of both transverse energy and variable (22) to decrease below zero. However, another condition of the distribution function (23) nullification at some $\varepsilon_{\perp max}$ or ξ'_{max}, essential for the present approach [10,13], needs some comments. Indeed, at first glance, the region of large $\varepsilon_\perp$ is surely well populated by the intensively scattering dechanneling particles. However, the diffusion equation is applicable in the limit of small changes of the considered quantity, transverse energy in our case. That is why one should adopt that at some $\varepsilon'_\perp$ or ξ'_{max}, when the variation

$$\delta\varepsilon_\perp(\varepsilon') = \left(\left\langle \frac{(\Delta\varepsilon_\perp)^2(\varepsilon'_\perp,x)}{\Delta z} \right\rangle T(\varepsilon') - \left\langle \frac{\Delta\varepsilon_\perp(\varepsilon'_\perp,x)}{\Delta z} \right\rangle^2 T^2(\varepsilon'_\perp) \right)^{1/2} \quad (28)$$

of the former over the channeling period reaches the interval $V_{max} - \varepsilon'_\perp$, separating $\varepsilon'_\perp$ from the potential maximum, equation (24) ceases to describe any particle, justifying thus the second boundary condition $u(\xi'_{max}) = 0$, where $\xi'_{max} = \xi'(\varepsilon_{\perp max})$ and $\delta\varepsilon_\perp(\varepsilon_{\perp max}) = V_{max} - \varepsilon_{\perp max}$. To estimate the uncertainly of this definition of $\varepsilon_{\perp max}$, we took the ratios

$$\delta\varepsilon_\perp(\varepsilon_{\perp max})/\left[V_{max} - \varepsilon_{\perp max}\right] = 0.5,\ 1,\ 2,$$

to demonstrate in Table 1 that an uncertainty of the dechanneling length definition is marginal.

Given the boundary value ξ'_{max}, one can redefine Eq. (24) to formulate Sturm-Liouville problem on the interval $[0,1]$ of the normalized variable $\xi = \xi'/\xi'_{max}$ by omitting the prime in Eqs. (23)-(27) and putting $p'(\xi) = p(\xi)\xi'^2_{max}$:

$$r(\xi)\frac{\partial u(\xi,z)}{\partial z} = \frac{\partial}{\partial\xi}\left(p(\xi)\frac{\partial u(\xi,z)}{\partial\xi}\right) - q(\xi)u(\xi,z) , \quad (29)$$

$$-\frac{\partial}{\partial\xi}\left[p(\xi)\frac{\partial}{\partial\xi}u_n(\xi)\right] + q(\xi)u_n(\xi) = \lambda_n r(\xi)u_n(\xi), \quad (30)$$

$$\partial u_n(0)/\partial\xi = 0, \quad u_n(1) = 0, \quad n = 1,2,.., \quad (31)$$

where we follow the sign convention of [20]. The dependence of the Eqs. (29), (30) coefficients on the normalized parameter ξ is illustrated by Fig. 2 in the case of 400 GeV protons and (110) Si planes, also used as an example in Figs. 3-7 below.

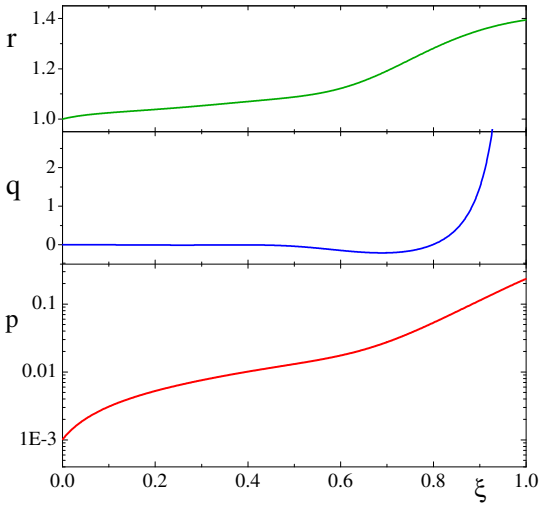

Fig. 2. The Eqs. (29) and (30) coefficient dependence on the parameter ξ for 400 GeV protons channeled by the (110) Si planes.

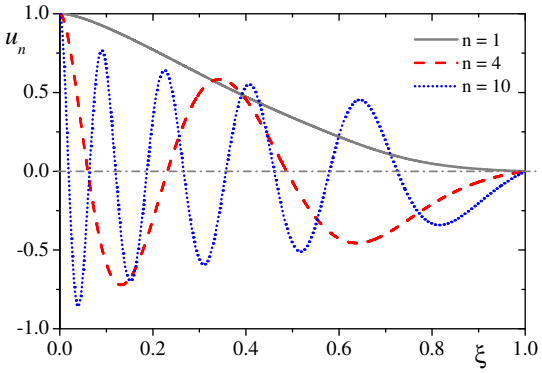

Fig. 3. The 1-t, 4-th and 10-th eigen states for the same.

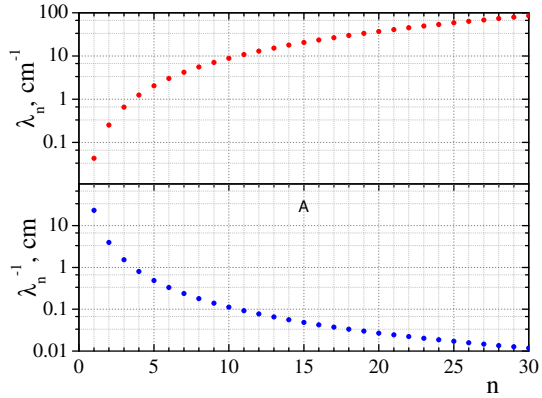

Fig. 4. The eigen values of Eq. (30) (top) and corresponding decay lengths (bottom).

3 Diffusion equation solution and its analysis

3.1 Dechanneling length at different energies

A numerical solution of Sturm-Liouville problem (30), (31), like that of [20], allows one to find any number of its eigen

Table 1. Dechanneling length and precision of its evaluation

Potential	$\frac{\delta\varepsilon_\perp(\varepsilon_{\perp\max})}{V_{\max}-\varepsilon_{\perp\max}}$	$l_{dech},\ cm$	$\Delta l_{dech},\%$
Tob [14]	1	**23.1**	**0**
Tob [14]	0.5	22.9	-0.81
Tob [14]	2	23.2	+0.37
DT [15]	1	23.3	+0.61
Mol [7]	1	21.4	-7.255

states $u_n(\xi)$ and eigen values λ_n, $n = 1, 2, ..$, some of the lowes of which are plotted, respectively, in Figs. 3 and 4. The eigen values λ_n are positive and monotonically increase with their numbers n, equal to the number of corresponding eigen state $u_n(\xi)$ nodes minus one. The completeness property of the system of eigen states of the problem (30), (31) allows one to represent any solution of Eq. (29) in the form of expansion

$$u(\xi, z) = \sum_{n=1}^{\infty} c_n \exp(-\lambda_n z)\, u_n(\xi), \tag{32}$$

the coefficients c_n of which are determined by the distribution $u(\xi, 0)$ at the crystal entrance $z = 0$ and are evaluated below. The solution (32) allows one to determin the channeling probability dependence on crystal depth

$$P_{ch}(z) \equiv \frac{N_{ch}(z)}{N_0} = \int_0^1 u(\xi, z)d\xi = \frac{1}{N_0}\sum_{n=1}^{\infty} N_{n0}\exp(-\lambda_n z) = \sum_{n=1}^{\infty} c_n\bar{u}_n \exp(-\lambda_n z) \overset{z\lambda_1>1}{\longrightarrow} c_1\bar{u}_1\exp(-\lambda_1 z), \tag{33}$$

where

$$\bar{u}_n = \int_0^1 u_n(\xi)d\xi. \tag{34}$$

An exponential decay of the eigen states is governed by their eigen values, the smallest first of which alone determines the asymptotic exponential behavior of the general solution (32), which gave rise to the introduction of the dechanneling length $l_{dech} = 1/\lambda_1$ in [10]. Uncertainties of the latter, connected with both the qualitative nature of the introduction of the boundary $\varepsilon_{\perp max}$ of the diffusion approximation applicability region and the planar potential model, are displaced in table 1 for 400 GeV protons and (110) Si planes. As one can see, both the uncertainty of the boundary energy $\varepsilon_{\perp max}$ definition and the transition between the potential models [22] and [21] change the l_{dech} value by less then one percent. Considerably smaller dechanneling length, obtained with the Moliere potential [9], reflects the limited applicability of the latter to the channeling phenomenon. In any case, the precision of l_{dech} determination by the diffusion equation method is not worse than the uncertainty related with the potential model choice.

Table 2 displays the l_{dech} values for both positively and negatively charged ultra-relativistic particles demonstrating the large value of the ratio $\lambda_2/\lambda_1 \sim 6 \div 8$, assuring the strong dominance of the first eigen state starting from $z \sim l_{dech}$ (see below).

Table 2. Dechanneling lengths for protons and electrons of different energies

e^-/p	ε, GeV	l_{dech}, cm	λ_2/λ_1	Δl_{dech}, %	N_{ch0}/N_0
p	400	23,1	6.0	0.61	0,895
p	6500	303.6	5.7	0.34	0.895
p	10^5	3936.0	5.6	0.18	0.895
e^-	1	6.0 10^{-4}	7.8	130.0	0.33
e^-	10	50.0 10^{-4}	6.9	78.0	0.39
e^-	100	0.044	6.4	46.0	0.44
e^-	1000	0.38	6.1	28.5	0.49

3.2 Nuclear dechanneling probability dependence on particle penetration depth

However the evolution of the probability (33) at the smaller depths $z \leq l_{dech}$ is governed by many states, making its behavior more complex. To study an interference of different eigen states, one should know their amplitudes $c_n\bar{u}_n$ (see Eq. (33)). The simplest formula can be obtained for them in the limit of zero particle incidence, when $|d\varepsilon_\perp| = |dV(x)/dx|dx$ and the distribution function at the crystal entrance reduces to

$$u(\xi, 0) = \frac{1}{N}\frac{dN}{d\xi} = \frac{\xi'_{max}}{d_{pl}T\left(\varepsilon_\perp(\xi)\right)\left|dV\left(x\left(\varepsilon_\perp(\xi)\right)\right)/dx\right|}, \tag{35}$$

allowing one to evaluate both the coefficients

$$c_n = \int_0^1 u(\xi, 0)u_n(\xi)r(\xi)d\xi \left(\int_0^1 u_n^2(\xi)r(\xi)d\xi\right)^{-1} = \int_0^d u_n\left(\xi(V(x))\right)r\left(\xi\left(V(x)\right)\right)\frac{dx}{d}\left(\int_0^1 u_n^2(\xi)r(\xi)d\xi\right)^{-1} \tag{36}$$

of the expansion (32) and the amplitudes $N_{n0}/N_0 = c_n\bar{u}_n$ of the eigen states, which enter Eq. (33) and are plotted in Fig. 5.

Eqs. (33) and (36) allow one to illustrate the main features of the dechanneling process of positively charged particles in the most practically important and complex region $l < l_{dech}$. Since only the particles with sufficiently high transverse energies reach the regions of atomic nuclei localization (see Fig. 1), the fast nuclear and slow electron dechanneling processes, which dominate, respectively, at sufficiently high and low transverse energies, can be qualitatively distinguished. The question arises, however, is it possible to strictly introduce and measure both the nuclear and electron dechanneling lengths, as was done in [14,15]? It is the knowledge of both the eigen values and the amplitudes (36) of eigen states, entering the solution (32), which make it possible to treat this question thoroughly.

Fig. 4 shows that the number of the eigen values, the inverse values of which correspond to the typical nuclear

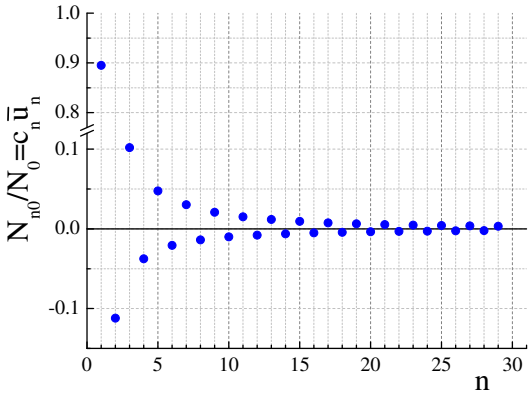

Fig. 5. The eigen state amplitudes entering Eq. (33).

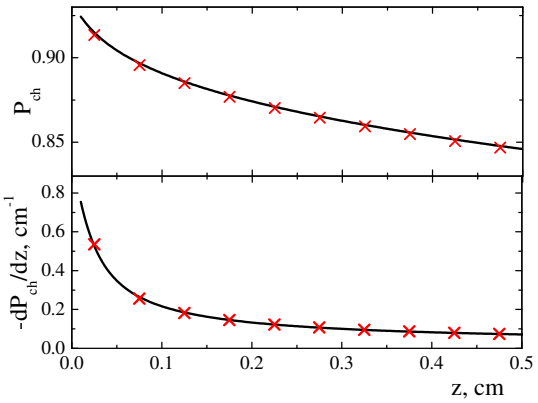

Fig. 6. Crystal depth dependence of the channeling probability (33) (solid line, top) and dechnneling rate (solid line, bottom) and their fits by the function (37) and its derivative, taken with the negative sign, respectively (crosses).

dechanneling region (about $1mm$ at $400GeV$), exceeds one considerably. Corresponding eigen states also have the amplitudes, comparable in value. The cumulative contribution of these multiple and close fast decaying states is approximated by the integral of the exponent $\exp(-\lambda(\varepsilon_\perp)z)$ product by a slowly varying function of transverse energy well fitted by the power-type

$$P_{ch}(z) = \sum_{n=1}^{\infty} c_n \bar{u}_n \exp\left(-\lambda_n z\right) \overset{z\ll\lambda_1}{\longrightarrow} 0.954 - 0.137\sqrt[3]{z}, \tag{37}$$

instead of exponential-type function of the crystal depth z, as Fig. 6 demonstrates. Thus, in place of the dechanneling length extraction, the experiments on nuclear dechanneling should accept the power-type fiting of the channeling fraction dependence on depth.

3.3 Peculiarities of the electron dechanneling of positively charged particles

On the opposite, a few lowest eigen values, describing the electron dechanneling process, differ severalfold – see Fig. 4. In addition, the smallest first of them possesses an especially large amplitude $N_{10}/N_0 = c_1\bar{u}_1$ – see Fig. 5. By

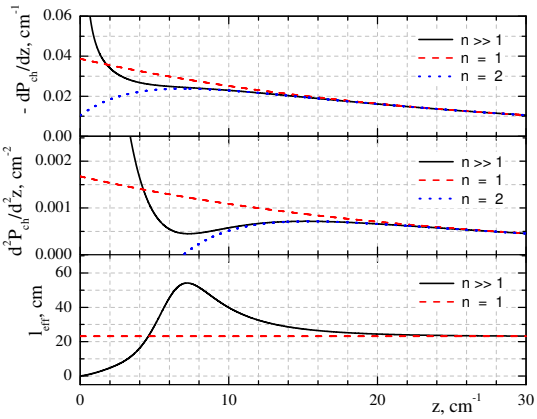

Fig. 7. Dechanneling rate (38), its derivative (39) and effective decahnneling length (40) versus crystal depth.

this reason the applicability of the electron dechanneling length notion is assured starting just from $z \simeq l_{dech} = 1/\lambda_1$. However the real experiments on beam steering, collimation and electromagnetic radiation generation are conducted at $z < l_{dech}$ and even at $z \ll l_{dech}$, where several lowest eigen state contribute considerably to both Eq. (32) and (33), violating their asymptotic exponential behavior. Indeed, let us consider both the dechanneling rate

$$-P'_{ch}(z) = \sum_{n=1}^{\infty} c_n \bar{u}_n \lambda_n \exp\left(-\lambda_n z\right), \tag{38}$$

which can be measured experimentally, and its derivative

$$P''_{ch}(z) = \sum_{n=1}^{\infty} c_n \bar{u}_n \lambda_n^2 \exp\left(-\lambda_n z\right) \tag{39}$$

(see Fig. 7). The point is that the relatively small population coefficients $|c_n| \ll c_1$ with $n > 1$ are multiplied by the large eigen values $\lambda_n \gg \lambda_1$ and their squares in Eqs. (38) and (39), respectively, making their "weights" comparable with that of the first eigen state. Having, in addition to its high "weight", the negative sign of the amplitude, the second eigen state directly distorts the steady decrease of the leading contribution of the latter. To demonstrate how the states with $n > 1$ modify the exponential channeling decay law at $z < l_{dech}$, let us introduce the effective dechanneling length

$$l^{eff}_{dech}(z) = -\frac{P'_{ch}(z)}{P''_{ch}(z)}. \tag{40}$$

The latter is equal to the constant quantity $l_{dech} = 1/\lambda_1$, either when only the first terms in the sums (38) and (39) are preserved or if the region $z \gg l_{dech}$ is considered. However at $z < l_{dech}$ the $n > 1$ terms induce the considerable dependence of the effective dechanneling length (40) on depth, resulting in its doubling at $z = 6 \div 8cm$ – see Fig. 7. That is why, instead of fitting the data by the single exponent containing a constant electron dechanneling length, more complex behavior of the dechanneling process of positively charged particles should be considered to

establish the the crystal thickness, optimal for the applications. One of the most fundamental one of the channeling in thick crystals is the measurement of both magnetic and electric dipole momenta of short living particles [7].

3.4 Diffusion equation application to the dechanneling of negatively charged particles

Since the particle scattering by nuclei is thoroughly taken into consideration by Eqs. (29) and (30), the solution (32) can be also applied to the case of negatively charged particles. Oppositely to the case of positively charged ones, all negatively charged particles experience strong nuclear scattering, inducing large fluctuations of transverse energy at any value of the latter. As a result, more than 50% of the particles (see table 2), having transverse energies $\varepsilon_{\perp max} < \varepsilon_{\perp} \leq V_{max}$, experience average transverse energy variations (28) exceeding the depth $V_{max} - \varepsilon_{\perp max}$ of their transverse energy level occurrence. These variations induce either immediate dechanneling or large changes of both the transverse motion period and phase, making, in fact, inapplicable the whole notion of channeling, understood as a quasiperiodic transverse motion. The rest of the particles with $\varepsilon_{\perp} < \varepsilon_{\perp max}$, which more likely can be considered as channeled, also experience large transverse energy fluctuations resulting in the uncertainly of dechanneling length which reaches several tens of percent – see table 2.

Contrary to the case of positively charged particles, nuclear scattering of negatively charged ones, which occurs near the potential energy minimum, can immediately make their transverse energy considerably less than the height of the potential barrier, giving rise to the intensive reachanneling process which Eqs. (29), (30) are unable to describe. Thus, in total, the diffusion equation approach provides merely qualitative information on the dechanneling process of negatively charged particles. Taking into consideration that the dechanneling length of negatively charged particles is much less than that of positively charged ones (see table 2), one should acknowledge the Monte Carlo simulations to be a quite adequate approach for negatively charged particle dynamics study. In particular, this method correctly reproduces the nearly exponential decay of the channeling population in a bent crystal observed in [12], to describe which the diffusion equation should be additionally refined.

Monte Carlo simulations also certainly take into consideration all possible features of positively charged particle motion. In particular, they correctly describe both the rechanneling process and the large transverse energy fluctuations at the upper under-barrier region $\varepsilon_{\perp} \sim \varepsilon_{\perp max}$, in which the diffusion equation looses its applicability. Monte Carlo approach have also demonstrated its efficiency in simulation of the new effects of channeling probability increase by the crystal cut [23], positive miscut influence of collimation [24] and other possibilities of the latter [25], multiple new radiation features in both crystal undulators [2,26,27] and bent crystals [28,29], the effects of planar channeling and quasichanneling oscillations in the deflection angle distribution of particles passed through a bent crystal [30] and many effects in the field of atomic strings [31,32,33,34,35,36,37]. However the main purpose of this paper was to demonstrate that despite all the achievements of Monte Carlo method, the diffusion equation approach, refined in present paper, can supplement the simulation results with the enlightening treatment of the collective statistical behavior of channeling particles, which can not be described by the sum of two exponents decaying with nuclear and electron dechanneling lengths.

Both electron and nuclear dechanneling lengths can be measured using bent crystals [14,15,16]. Crystal bending will certainly change the dechanneling length values from table 2, evaluated for a straight crystal. Though both experiment and simulations demonstrate reasonable applicability of thee dechanneling length of electrons in bent crystals [12], to predict its value diffusion equation (7) should be further expanded to take into consideration the strong rechanneling effect. On the opposite, a marginal role of the rechanneling process of positively charged particles allows one to assume that the new conclusions concerning the dechanneling rate dependence on crystal depth remain true also at the presence of crystal bending and should be used to reinterpret the results of the experiments of the [14,15,16] type.

4 Conclusions

In this paper the equation of channeling particle diffusion in transverse energy was supplemented with the effect of nuclear scattering and applied for a direct evaluation of the huge dechanneling length values at the multi-TeV particle energies. The diffusion equation approach has also proved to be really indispensable in revealing the general features of the collective statistical behavior of channeling particles such as the power-type channeling probability dependence on the particle penetration depths in the nuclear dechanneling region and a strong dependence of the effective electron dechanneling length on the particle penetration depth in the interval between the nuclear dechanneling region and approximately one electron dechanneling length. These fundamental predictions, which strongly contradict the straightforward application of both nuclear and electron dechanneling lengths, should be used for an unbiased interpretation of the simulation predictions and represent themselves a challenge for the future experiments.

References

1. V.G. Baryshevsky. *High-Energy Nuclear Optics of Polarized Particles* (World Press, 2012).
2. V.G. Baryshevsky, V.V. Tikhomirov, Nucl. Instrum. And Methods. B **309**(2013) 30.
3. A.V. Korol, A.V. Solov'yov and W. Greiner. Channeling and Radiation in Periodically Bent Crystals (Springer Series on Atomic, Optical and Plasma Physics 69).

4. W. Scandale, Mod. Phys. Lett. **A27**, (2012)1230007.
5. V. M. Biryukov, Y. A. Chesnokov, V. I. Kotov *Crystal Channeling and Its Application at High-Energy Accelerators* (Springer-Verlag, Berin and Heidelberg GmbH & Co. K, 2010).
6. F. Zimmermann, Nuclear Instrum. and Meth. B. **B355**, (2015) 4-10.
7. F.J. Botella et al., (preprint) http://arxiv.org/pdf/1612.06769v1.pdf
8. J. Lindhard, Mat.-Fys. Medd. Dan. Vid. Selsk. **34**, (1965) 1-64.
9. D.S. Gemmel. Rev. Mod. Phys. **46**, (1974) 129.
10. V.V. Beloshitsky, M. A. Kumakhov, V. A. Muralev, Radiation Effects. **20**, (1973) 95-109.
11. V.V.Tikhomirov, Nucl. Instrum. and Meth. **B36**, (1989) 282-285.
12. A. Mazzolari et al., Phys. Rev. Lett. **112**, (2014) 135503.
13. V.M. Biryukov et al., Nuclear Instrum. and Meth. B. **B86**, (1994) 245-250.
14. W. Scandale et al., Phys. Lett. B. **680**, (2009) 129132.
15. E. Bagli et al., Eur. Phys. J. C **74**, (2014) 2740.
16. W. Scandale et al., Phys. Lett. B. **719**, (2013) 7073.
17. E.M.Lifshitz, L.P. Pitaevskii, *Physical Kinetics*. Vol. 10 . Pergamon Press. 1981.
18. V. N. Baier, V.M. Katkov, V.M. Strakhovenko, *Electromagnetic Processes at High Energies in Oriented Single Crystals* (World Scientific, Singapore. 1998).
19. N. M. Matveev, *Methods for integration of the ordinary differential equations*. (Vysshaja shkola, Moskva, 1967). (in Russian).
20. S. Pruess, C.T. Fulton, ACM Transactions on Mathematical Software **19**, (1993) 360-376.
21. M.Tobiyama et al., Phys. Rev. B. **44**, (1991) 9248-9258.
22. P.A. Doyle, P.S. Turner, Acta Crystallog **24A**, (1968) 390-397.
23. V.V. Tikhomirov, JINST **2**, (2007) P08006.
24. V.V. Tikhomirov and A.I. Sytov, Nucl. Phys. Invest. (Kharkov) **57**, (2012) 88-92.
25. A.I. Sytov, V.V. Tikhomirov, Nucl. Instrum. And Methods. B. **355**, (2015) 383386.
26. E. Bagli et al., Eur. Phys. J. C **74**, (2014) 3114.
27. V.V. Tikhomirov, (preprint) http://arxiv.org/pdf/1502.06588v1.pdf
28. V. Guidi, L. Bandiera and V.V. Tikhomirov, Phys. Rev. A **86**, (2012) 042903.
29. L. Bandiera et al., Phys. Rev. Lett. **115**, (2015) 025504.
30. A.I. Sytov et al., Eur. Phys. J. C **76**, (2016) 77.
31. V.V. Tikhomirov, Phys. Lett. B. **655**, (2007) 217-222.
32. W. Scandale et al., Phys. Lett. B **682**, (2009) 274-277.
33. W. Scandale et al., Europhysics Lett. **93**, (2011) 56002.
34. L. Bandiera et al., Nucl. Instrum. And Methods. B **309**, (2013) 135-140.
35. V. Guidi, A. Mazzolari, V.V. Tikhomirov, J. Appl. Phys. **107**, (2010) 114908.
36. L. Bandiera et al., Phys. Rev. Lett. **111**, (2013) 255502.
37. V.V. Tikhomirov, A.I. Sytov, Nucl. Instrum. And Methods. B. **309**, (2013) 109-114.